Modified particle swarm optimization with chaotic attraction strategy for modular design of hybrid powertrains

Zhou, Quan; He, Yinglong; Zhao, Dezong; Li, Ji; Li, Yanfei; Williams, Huw; Xu, Hongming

DOI:
10.1109/TTE.2020.3014688

Modified Particle Swarm Optimization with Chaotic Attraction Strategy for Modular Design of Hybrid Powertrains

Quan Zhou, *Member, IEEE*, Yinglong He, Dezong Zhao, Senior *Member, IEEE*, Ji Li, *Member, IEEE*, Yanfei Li, Huw Williams, and Hongming Xu*

Abstract **— This paper proposes a new modular design method for hybrid powertrains using a modified accelerated particle swarm optimization (MAPSO) algorithm. The method determines the optimal combination of component specifications and control parameters, where the component specifications include integer variables (e.g. the number of battery modules). A unified chaotic attraction strategy for MAPSO is developed based on a logistic map to improve the probability of achieving the global optimal result. Pareto analysis is carried out to identify the weighting value for the trade-off in modular design. The Comprehensive Reputation Score (CRS), considering both Monte Carlo results and the probability of achieving global optima, is employed to evaluate the advantageous of the MAPSO compared to conventional PSO and four other PSO variants. The MAPSO is verified as the best because it has the highest CRS. Both two-level and simultaneous methods for modular design are developed with the MAPSO, where the former firstly operates component sizing at the level-1 and then conducts control optimization at the level-2, the later optimizes the size and control simultaneously. Compared to the two-level method, the simultaneous method achieves 7% higher cost function value and saves 50% time.**

Index Terms**— Modular design; Hybrid vehicle; Particle swarm optimization; Chaotic attraction; Integer variables**

I. INTRODUCTION

Growing concerns for air quality and the advent of zero-emission zones have motivated the automotive industry to seek low-cost carbon emission reduction solutions [1], [2]. The hybridization of vehicles offers a promising solution to energy saving and emissions reduction. Thermal propulsion systems will experience a transition from being the 'solo' propulsion device to being part of a 'hybrid' system [3]–[5].

Powertrain optimization is critical for the success of hybrid vehicles [6]. Both online and offline optimization methods are being developed to minimize fuel consumption, emissions and cost [7], [8]. Model-based predictive control [9], [10], equivalent consumption minimization strategy [11], [12], and reinforcement learning [13]–[15] have been applied to online optimize energy flows of the vehicle. On the other hand, offline optimization is essential to guarantee the optimal settings of component size and control parameters [16], [17]. It is because changing some key parameters (e.g. engine displacement) is almost impossible once they have been fixed for production.

Modular design allows fast and low-cost development of new vehicular products [18]. Volkswagen develops a modular platform for the flexible development of its new electric and hybrid powertrains [19]. CHANGAN motor unveiled its brandy new 'Blue Core' high-efficiency internal combustion engine (ICE) series for hybrid vehicles on a modular platform [20]. Modular design is also widely accepted for the development of off-highway vehicles [21]. Conventionally, the modular design relies on the engineers' experience, while the design results are determined by the design of experiments (DoE) [22]. Artificial intelligence has been deployed for hybrid vehicles for global optimization [23], and this motivates the research into intelligent modular design. Intelligent modular design of hybrid powertrain is an offline optimization problem on the system level, and there are two typical methods [24], i.e. two-level and simultaneous optimizations.

Two-level optimizations consider component sizing and control optimization as two separated tasks. For component sizing, Pourabdollah et al. optimized a hybrid vehicle based on varying levels of modelling details using Convex Optimization (CO) [25]. The optimal component size of a hybrid system considering the cost and battery life has been developed using the Nondominated Sorting Genetic Algorithm (NSGA-II) [26]. Shahverdi et al. obtained the Pareto frontier of component cost and fuel economy with a genetic algorithm [27]. Xu et al. used the exhaustive search method to optimize the topology of hybrid vehicles considering different powertrain layouts [28]. For control parameters, Wang et al. optimized the control parameters for energy management to minimize the daily cost using dynamic programming (DP) [29]. Lv et al. implemented a neural network driver model for control parameter calibration to allow personalized vehicle economy optimization [30].

Simultaneous optimization deals with the component sizing and control parameter optimization as an integrity. Lv et al. found the optimal combination of component size and control parameters considering the vehicle dynamic performance, ride comfort and energy efficiency [31]. Leahey et al. optimized the component size and control parameters of a hybrid vehicle using a scripted algorithm [32]. Mamun et al. determined the optimal component specification and control parameters of a vehicle using the particle swarm optimization (PSO) [33].

Two-level and simultaneous optimizations have been investigated in many different hybrid vehicle studies, but there is no evidence showing that there exists a universal optimization method for all scenarios [24]. On the other hand, most of the literature assumes that the design variables are continuously varying [34], [35]. The modular design must consider the design variables which are from discontinuously varying domains (e.g. integers). This motivates the development of modular design method based on the meta-heuristic algorithm as it does not require derivation information.

The authors have carried out a series of research on optimization methods for vehicle powertrains with meta-heuristic algorithms, including NSGA [36], SPEA [37], [38], and PSO [39], [40]. We chose the PSO variant for the intelligent modular design for the following two reasons: 1) PSO has fewer tuning parameters (compared to NSGA, SPEA); 2) PSO

requires low computational effort (compared to DP) [41] and is flexible for either two-level or simultaneous optimization. The Accelerated Particle Swarm Optimization (APSO) further reduces the number of attraction factors from 2 to 1 and has shown advantageous in global searching compared with conventional PSO [42]. Conventional APSO updates the position of its particles with the assumption that the design parameter candidates are continuously varying within their lower and upper boundaries [43]. This paper further develops a particle position updating strategy to enable optimal searching with mixed-integer variables for modular design.

Chaotic maps have shown the capability of tuning PSO parameters adaptively during the optimization process so that they can improve the convergence speed and the consistency of the optimization results in different trials [44]. Li et al. introduced a logistic map to tune the algorithm for gasoline engine optimization [45]. Yu et al implemented a variant of the logistic map (tent map) to tune the PSO parameters for air bearing optimization [46]. Logistic map [47], Gauss map [48], Singer map [49], and Sinusoidal map [50] have been widely studied for parameter tuning in PSO algorithms that deal with continuous-varying variables. However, a unified chaotic attraction strategy for modular design, which deals with mixed-integer variables, has not been reported yet.

To achieve the robustly optimal solution retrieving for module design of hybrid powertrains, this paper proposes a Modified Accelerated Particle Swarm Optimization (MAPSO) algorithm. This work aims to deliver two new main contributions: 1) The capability of optima searching in discrete-varying domains using the newly proposed MAPSO will be verified, which will resolve the modular design problem with mixed-integer variables; 2) A unified chaotic attraction strategy will be developed based on the logistic map, which tunes the attraction factor of the MAPSO adaptively during the optimization process in modular design. The advantageous of the proposed MAPSO will be evaluated compared with the conventional PSO and the APSOs with three commonly used chaotic maps. The evaluation will consider both Monte Carlo results and the probability of achieving global optima. The vehicle performance using the proposed algorithm for both two-level and simultaneous optimizations are demonstrated in both software-in-the-loop and hardware-in-the-loop tests.

The rest of the paper is organized as follows: Section II provides information about the off-highway vehicle system and the scalable powertrain modules. The optimization problem is formulated in Section III. The accelerated particle swarm optimization algorithm is modified for modular design in Section IV. Experiment platforms are introduced in Section V. The results of experiments are also presented and discussed in Section V. Conclusions are summarized in Section VI.

II. The Vehicle and Scalable Powertrain Modules

A. The Vehicle System

This paper demonstrates the intelligent modular design of a hybrid aircraft-towing tractor, as in Fig. 1. The tractor has a series hybrid powertrain using a 245kW traction motor, which is powered by a battery pack, and an engine-generator that provides extra power for vehicle operation and battery charging. The energy management controller determines the amount of power contributed by the engine-generator and the battery package to satisfy the power demand and maintain the battery state of charge (SoC). Parameters of the vehicle are listed in Table I and the vehicle is modelled in Appendix I.

Fig. 1. The hybrid aircraft-towing tractor system

Table I. Vehicle Parameters

Parameter	Description	Value
m_{veh}	Vehicle mass	16t
r_{whl}	Radius of the wheels	0.75m
f_f	Friction coefficient	0.02
C_d	Aerodynamic drag coefficient	0.8
A_f	Effective front area	6.8m^2

B. Scalable Powertrain Modules

Scalable modules, including an engine-generator module, a battery module, and an energy management module, will be optimized in this paper to allow a hybrid powertrain achieving its maximum energy efficiency with the minimum geometric size. The engine-generator module and battery module are modelled based on the datasheets provided by the suppliers [51] [38]. The energy management module is developed using a widely used power-distribution function.

1) Engine-generator module

The engine-generator module consists of an ICE, a generator, and a fuel tank. The engine model is based on Williams' approximation [26] and assumes a constant bore-to-stroke ratio. The equivalent power of the fuel consumption is scaled by the displacement of the engine L_{ice}

$$P_{\text{fuel}}(t, L_{\text{ice}}) = \frac{L_{\text{ice}}}{L_{\text{ref}}} \cdot H_f \cdot \dot{m}_f(u_{\text{egu}}(t)) \quad (1)$$

where L_{ice} is the displacement of the candidate engine in litres; L_{ref} is the displacement of the baseline engine in litres. In this work, a 4.4L diesel engine is selected as the baseline. Here $\dot{m}_f$ is represented by the fuel consumption map, which is based on the engine generator control command $u_{egu}(t)$, and H_f is the heat value for the diesel fuel, which is 44×10^6J/kg.

The dimensional size of the engine generator vol_{egu} is scaled using a logistic function of the engine displacement L_{ice}

$$vol_{\text{egu}}(L_{\text{ice}}) = \frac{1}{c_{\text{e1}} + e^{-(c_{\text{e2}} \cdot L_{\text{ice}} + c_{\text{e3}})}} \quad (2)$$

where $c_{\text{e1}} = 9.5\text{e}-5$, $c_{\text{e2}} = 0.9006$, and $c_{\text{e3}} = 5.685$ are the model parameters, which are calibrated using the MATLAB curve fitting toolbox based on a dataset from the supplier [51].

2) Battery module

Each battery module is assembled by arranging 100 Panasonic 18650 battery cells in series to achieve a nominal voltage of 370V. A 2-RC battery model is developed and calibrated with the data from [52]. The battery pack is scaled by the total number of the battery module in parallel, n_{bm}. The power loss of the battery is

$$P_{\mathrm{batt\_loss}} = n_{\mathrm{bm}} \cdot R_{\mathrm{eqv}}(\mathrm{t}) \cdot {I^2}_{\mathrm{batt}}(t) \tag{3}$$

where R_{eqv} is the battery internal resistance derived from the battery's SoC. In practice, the battery SoC is observed by the battery voltage $U_{\mathrm{batt}}(t)$, and the current $I_{\mathrm{batt}}(t)$. Therefore, in this paper, the battery internal resistance is mapped by the battery voltage and current, i.e. $R_{\mathrm{eqv}}(U_{\mathrm{batt}}(t), I_{\mathrm{batt}}(t))$.

The dimensional volume of the battery package vol_{bp} is scaled by the number of Lithium-ion battery cells n_{bc} as

$$vol_{\mathrm{bp}}(n_{\mathrm{bm}}) = n_{\mathrm{bm}} \cdot 100 \cdot 4 \cdot {r_{\mathrm{cell}}}^2 \cdot h_{\mathrm{cell}} \tag{4}$$

where r_{cell} is the radius of the battery cell; and h_{cell} is the height of the battery cell. In this work, r_{cell} and h_{cell} are set as 6.5×10^{-3}m and 65.3×10^{-3}m, respectively [52].

3) Energy management module

The power supplied by the engine generator and battery is calculated in real-time by

$$\left.\begin{aligned} P_{\mathrm{egu}} &= u_{\mathrm{egu}}(SoC) \cdot P_{\mathrm{egu\_max}} \\ P_{\mathrm{batt}} &= P_{\mathrm{dem}} - P_{\mathrm{egu}} \end{aligned}\right\} \tag{5}$$

where P_{batt} is the power supplied by the battery pack and P_{egu} is the power supplied by the engine generator; $P_{\mathrm{egu\_max}}$ is the maximum power that can be provided by the engine-generator; and P_{dem} is the vehicle's power demand.

Energy management strategies, including exponential functions [7], model-based predictive control [9], [10], and model-free control [13], [14], build a nonlinear relationship between the power distribution and the vehicle states (e.g. battery SoC). This paper provides a paradigm based on the exponential function because it is robust and provides nonlinear constraints like the other strategies. The engine generator is therefore controlled by [23]

$$u_{\mathrm{egu}}(SoC) = \begin{cases} 0 & SoC\epsilon[0.8\ 1] \\ e^{\left(-\frac{(SoC-SoC^-)^2}{2\cdot {c_{\mathrm{ems}}}^2}\right)} & SoC\epsilon[0.2\ 0.8) \\ 1 & SoC\epsilon[0\ 0.2) \end{cases} \tag{6}$$

where c_{ems} is the control parameter to be optimized for power distribution control; SoC is the state of charge of the battery; and SoC^- is the lower battery SoC boundary. Normally $SoC^- = 0.2$ is chosen to ensure the battery health.

III. The Optimization Problem

The modular design aims to find the optimal combination of components size and energy management parameters. The mathematic model of the modular design is

$$\left.\begin{aligned} [L^*_{\mathrm{ice}} \quad n^*_{\mathrm{bm}} \quad c^*_{\mathrm{ems}}] &= \arg\min(J_{\mathrm{loss}} \quad J_{\mathrm{size}}) \\ \text{s.t.} &\begin{cases} L_{\mathrm{ice}} \in \boldsymbol{\mathcal{L}} \\ n_{\mathrm{bm}} \in \boldsymbol{\mathcal{N}} \\ c_{\mathrm{ems}} \in \boldsymbol{\mathcal{C}} \end{cases} \end{aligned}\right\} \tag{7}$$

where L^*_{ice} is the optimal engine size; n^*_{bc} is the optimal size of the battery package; c^*_{ems} is the optimal coefficient value for the power distribution function; $\boldsymbol{\mathcal{L}}$, $\boldsymbol{\mathcal{N}}$, and $\boldsymbol{\mathcal{C}}$ are the value domain of L_{ice}, n_{bm}, and c_{ems}, where $\boldsymbol{\mathcal{L}} = \{2.0, 2.1, 2.2, \dots, 6.0\}$, $\boldsymbol{\mathcal{N}} = \{55, 56, 57, \dots, 150\}$, and $\boldsymbol{\mathcal{C}} = \{c_{\mathrm{ems}} | 0.05 \le c_{\mathrm{ems}} \le 0.2\}$.

The first optimization objective J_{loss} is to minimise the total energy loss over a driving cycle, which can be calculated using the equivalent energy of both fuel consumption and the energy loss in the internal resistance of battery

$$J_{\mathrm{loss}} = \int_{t_0}^{t_p} P_{\mathrm{fuel}}(t) \cdot dt + \int_{t_0}^{t_p} P_{\mathrm{batt\_loss}}(t) \cdot dt \tag{8}$$

where P_{fule} and $P_{\mathrm{batt\_loss}}$ are calculated by Eq. (1) and (3).

The dimensional volume of components is considered in the second optimization objective, which is given by

$$J_{\mathrm{size}} = vol_{\mathrm{egu}}(L_{\mathrm{ice}}) \cdot 10^{-3} + vol_{\mathrm{bp}} \tag{9}$$

where vol_{egu} is the total volume of engine-generator that is calculated by Eq. (2); the volume of engine-generator is multiplied by 10^{-3} to convert the unit from L to m^3; vol_{bp} is the volume of battery pack calculated by Eq. (4).

IV. Modified Accelerated Particle Swarm Optimization Algorithm for Modular Design

This section introduces the idea of the modified accelerated particle swarm optimization (MAPSO) algorithm for modular design of hybrid powertrain for both simultaneous and two-level methods, where the new particle position updating strategy and chaotic attraction strategy are newly developed.

A. General Idea

The general idea of the module design with MAPSO algorithm is using the particle swarm intelligence to retrieve the best position (defined in a Euclidean coordinator compromising the variables needed to be optimized) that achieve the lowest cost in a nonlinear space (defined by the optimization objectives). The simultaneous method optimizes the design parameters and control parameters simultaneously as shown in Fig. 2. a). The two-level method optimizes the design parameters based on a guess control parameter on the first level and uses the optimized design parameters to find the optimal control parameters on the second level. The optimization results from the two-stage method will be found after several rounds of iteration with different initial guesses of control parameters.

The positions of particles (i.e. computing agents) are defined as following using a Euclidean coordinator

$$\left.\begin{aligned} \boldsymbol{x}_{i,j} &= [L_{\mathrm{ice}}, \quad n_{\mathrm{bm}}]^T \quad \text{lv. 1} \\ \boldsymbol{x}_{i,j} &= [c_{\mathrm{ems}}]^T \quad \text{lv. 2} \end{aligned}\right\} \text{two level}$$
$$\left.\begin{aligned} \boldsymbol{x}_{i,j} &= [L_{\mathrm{ice}}, \quad n_{\mathrm{bm}}, \quad c_{\mathrm{ems}}]^T \quad \text{simultaneously} \\ & i = 0,1,2,\dots,n;\ j = 1,2,..,p \end{aligned}\right\} \tag{10}$$

where $\boldsymbol{x}_{i,j}$ is the 'position' of the j^{th} 'particle' at i^{th} iteration; n is the maximum number of iterations, which is used to terminate the iterations; and p is the population of the particles, which defines the capability of global search in each iteration.

The objective function values are the total power loss $\boldsymbol{J}_{\mathrm{loss}}$ and the total volume of the powertrain components $\boldsymbol{J}_{\mathrm{size}}$, which is obtained by p cases of parallel simulations. A matrix of

particle positions $[\boldsymbol{x}_{i,1}, \boldsymbol{x}_{i,2}, \dots, \boldsymbol{x}_{i,p}]$ is the inputs of the parallel simulation. The simulation is based on the driving cycles that are defined with data from the London Heathrow Airport [17].

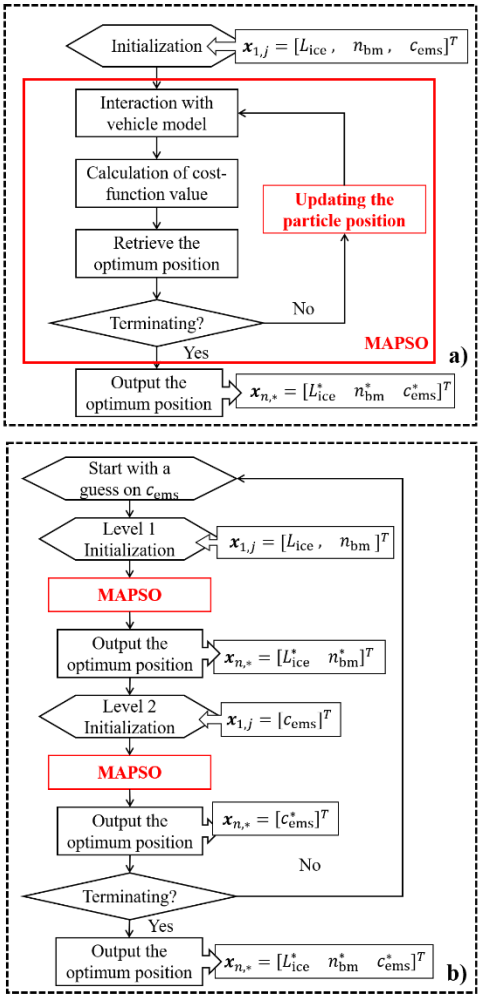

Fig. 2. Flow chart of the modular design with MAPSO: a) simultaneous method; b) two-level method

B. Particle Positions Update with a Floor Function

Conventional Accelerated Particle Swarm Optimization (APSO) algorithm updates the particle positions by

$$\boldsymbol{x}_{i+1,j} = \boldsymbol{x}_{i,j} + \beta \cdot (\boldsymbol{x}_{i,*} - \boldsymbol{x}_{i,j}) + \alpha^{i+1} \cdot \boldsymbol{r}_{i,j} \tag{11}$$

where $\boldsymbol{r}_{i,j}$ is a vector of unique random numbers for each particle in each iteration; α^{i+1} is a shrinking factor in reducing the influence of random moves; β is the attraction factor which controls how global best position will attract the movement of each particle. For standard APSO algorithm, the value of the attraction factor is fixed, and $\beta = 0.5$ is used [53]. $\boldsymbol{x}_{i,*}$ is the best position in i^{th} iteration, which is a column of the matrix $[\boldsymbol{x}_{i,1}, \boldsymbol{x}_{i,2}, \dots, \boldsymbol{x}_{i,p}]$ that satisfies

$$J(\boldsymbol{x}_{i,*}) \le J(\boldsymbol{x}_{i,j}) \tag{12}$$

where $i = 1,2, \dots, n$; $j = 1,2,..,p$. $J(\boldsymbol{x}_{i,j})$ is the cost function evaluated for each $\boldsymbol{x}_{i,j}$ value, which is calculated with a weighted-sum cost function to integrate the two objectives

$$J(\boldsymbol{x}_{i,j}) = \left(w \cdot \frac{J_{\text{loss}}(\boldsymbol{x}_{i,j})}{J^*_{\text{loss}}} + (1-w) \cdot \frac{J_{\text{size}}(\boldsymbol{x}_{i,j})}{J^*_{\text{size}}} \right) \tag{13}$$

where $\boldsymbol{x}_{i+1,j}$ and $\boldsymbol{x}_{i,j}$ are the position of the j^{th} particles at $i+1^{th}$ and i^{th} iteration respectively; w is the weighting factor; and J^*_{loss} and J^*_{size} are scale factors to ensure the values of the scaled objective functions are both within 0 and 1; J^*_{loss} is the energy loss determined by using a 6.0L engine-generator to track the tractor's power demand under the combined driving cycle; J^*_{size} is the total size of a 6.0L engine-generator and a battery pack with 150 modules that is calculated by Eq. (9).

To deal with the discontinuous variables for component sizing, i.e. for engine-generator $\boldsymbol{\mathcal{L}} = \{2.0, 2.1, 2.2, \dots, 6.0\}$ and for battery $\boldsymbol{\mathcal{N}} = \{55, 56, 57, \dots, 150\}$, the proposed Modified Accelerated Particle Swarm Optimization (MAPSO) algorithm modifies Eq. (13) as

$$\boldsymbol{x}_{i+1,j} = \frac{\text{floor}\,[s \cdot (\boldsymbol{x}_{i,j} + \beta \cdot (\boldsymbol{x}_{i,*} - \boldsymbol{x}_{i,j}) + \alpha^{i+1} \cdot \boldsymbol{r}_{i,j})]}{s} \tag{14}$$

where $\text{floor}(\text{x})$ is a function that rounds the elements of x to the nearest integers less than or equal to x; s is a scaling factor to generate new position with a resolution; s=1 is for battery module and s=10 is for engine-generator module because the displacement of the engine is varying with a resolution of 0.1.

C. Chaotic Attraction with Logistic Map

The general idea of chaotic attraction is to develop an iteration-variant attraction factor $\beta(i)$, which generates a set of $\beta \in [0,1]$ for each iteration, $\{\beta(1), \beta(2), \dots, \beta(n)\}$, to upgrade the attraction factor in β Eq. (13) and Eq. (14). Logistic map, which follows a principle of biological evidencing behavior, is proposed as a unified chaotic attraction strategy in this paper because it has only one tuning parameter and is easy to be implemented in engineering applications [47]. The logistic map dynamically updates the attraction factor in each iteration as

$$\beta(i) = \mu \cdot \beta(i-1) \cdot (1 - \beta(i-1)) \tag{15}$$

where μ is constant. According to the bifurcation diagram in Fig. 3. a), which illustrates the value of $\{\beta(2), \beta(3), \dots, \beta(n)\}$ with different settings of μ, $\mu = 4$ is chosen because it covers most values between 0 and 1. The β values in 50 iterations are shown in Fig. 3. b). The average β values (calculated with a moving window compromise 15 samples) are smaller than 0.5 in the first 25 interactions (to have more search around the local area) but are greater than 0.5 after the 25th iteration (to accelerate the convergence). This will theoretically prevent particles being trapped into local optima in a computationally effective way.

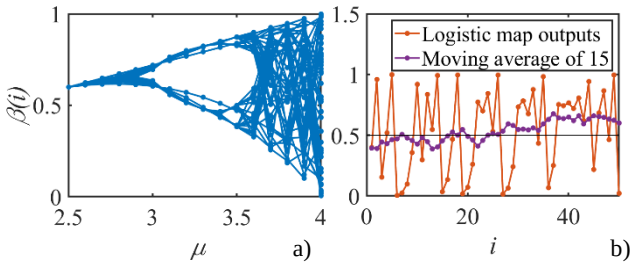

Fig. 3. Chaos behavior of logistic map: a) bifurcation diagram; b) dynamics in each iteration

V. Results and Discussion

The experimental study is carried out on both software-in-the-loop (offline) and hardware-in-the-loop (online) testing platforms. The MAPSO algorithm is initially running offline in MATLAB 2017a on a PC configured with an i7 CPU and 16GB RAM. Real-world cycles (RWC) 1-3 are defined using the data collected at the London Heathrow Airport on a tractor working with small, medium, and large airplanes, respectively. The combined driving cycle (CDC) is a random combination of RWC 1-3, which is used for offline optimization study. The driving cycle profile is illustrated in Table II. Both the CDC and RWC1-3 are used for the evaluation of the powertrain performance on the hardware-in-the-loop platform, as shown in Fig. 4. The performance of the powertrain using the optimized component parameters is emulated in the ETAS LABCAR, controlled by the ES910 with the optimized control parameter.

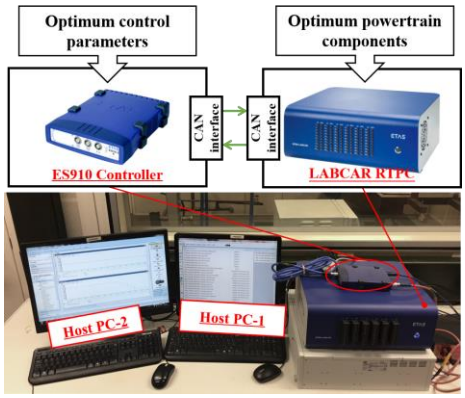

Fig. 4. Hardware-in-the-Loop testing facility

Table II. Summary of Driving Cycle Profiles

Algorithm	Comb. cycle	RWC-1	RWC-2	RWC-3
Cycle Length	8504s	4907s	4055s	4151s
Mean power demand	39.4kW	32.9 kW	35.5 kW	48.1 kW

A. Pareto Frontier for Selection of Weighting Factor

An approximated Pareto Frontier (aPF) for modular design under the combined driving cycle, as illustrated in Fig. 5, is obtained by calculating the nondominated set from the results obtained by the MASPO and the NSGA-II (a benchmark Pareto method) algorithms.

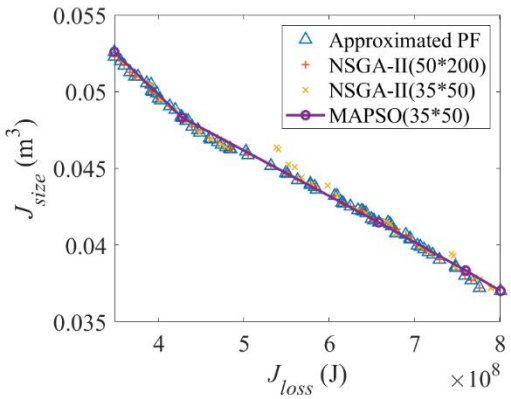

Fig. 5. Approximated Pareto Frontiers in modular design

The effectiveness of the estimated PF (ePF) obtained by the MAPSO (with different weighting factors) is validated by comparing it with the aPF and the ePF obtained by the NSGA-II algorithms with two different settings. A trade-off analysis based on the ePF will be conducted to guide the selection of the weighting factor of two optimization objectives in MAPSO.

The ePF obtained by the NSGA-II (50*200) algorithm, which has a population size (pop-size) of 50 running for 200 iterations, is shown in the red '+' sign. The ePT obtained by the MAPSO, which has a pop-size of 35 running for 50 iterations, is shown in purple circles. It illustrates the dominated optimum values of both objective functions (i.e. J_{loss} and J_{size}) with the weighting factor changing from 0 to 1 with a step size of 0.25. The weighting factor of 1 means the optimization only considers the energy loss while 0 means only the minimization of component size is considered. The ePF obtained by the NSGA-II (35*50), which has the same number of vehicle model iterations as the MAPSO, is shown in yellow 'x' sign. Error ratio, ER, and generational distance, GD, are used to evaluate the ePF obtained by the MAPSO and NSGA-II algorithms, which are defined by [54]

$$\left.\begin{aligned} \mathrm{ER} &= \frac{\sum_{m=1}^{N} e(y_m)}{N} \\ \mathrm{GD} &= \frac{\sqrt{\sum_{m=1}^{N} y_m \cdot \mathrm{dis}^2(y_m, \boldsymbol{S}_{\mathrm{aPT}})}}{N} \end{aligned}\right\} \tag{16}$$

where N is the member of elements in the ePF; y_m is the individual value in the ePF sets; $\boldsymbol{S}_{\mathrm{aPF}}$ is a set that forms the approximated Pareto Frontier (aPF); $e(y_m)$ =1 if $y_m \in \boldsymbol{S}_{\mathrm{aPF}}$ otherwise $e(y_m)$ =0; $\mathrm{dis}(y_m, \boldsymbol{S}_{\mathrm{aPF}})$ is the shortest distance between the element y_m and the aPF. The error ratio and generational distance of the MAPSO are compared with the NSGA-II methods in Table III.

Table III. Error Ratio and Generational Distance

Algorithm	MAPSO (35*50)	NSGA-II (35*50)	NSGA-II (50*200)
ER	0.80	0.68	0.94
GD	3.48×10^5	3.89×10^6	9.11×10^4

The ePF obtained by the MAPSO achieves higher ER and lower GD than the one obtained by the NSGA-II with the same number of vehicle model iterations. Although the ePF obtained by the NSGA-II (50*200) is better than MAPSO, it needs 10k vehicle model iterations that require more than 5 times of computational effort. In a consequence, the ePF obtained by the MAPSO is shown effective. Based on the ePF obtained by MAPSO, the energy loss can be reduced by 5% through increasing components size by 4% when the weight value changes from 0 to 0.25; and a 42% increase in component size can achieve a 56% energy loss reduction when the weight value changes from 0 to 1. The weighting value of 0.75 is chosen for the rest of the investigation because it saves 46% energy via the sacrifice of 30% increasing in powertrain size which has the highest energy-saving/volume-increasing ratio.

B. Comprehensive Reputation Evaluation

By running each of the modular optimization cases under the combined driving cycle using conventional PSO, conventional APSO, the proposed MAPSO, and the APSO with three other

CAS (i.e. Gauss map [48], Singer map [49], and Sinusoidal map [50]) for 20 times independently, statistical results of the cost-function values were obtained and are listed in 0.

Table IV. STATISTIC RESULTS OF 20 INDIVIDUAL OPTIMIZATION TESTS

Algorithm	J^*	Monte Carlo $\bar{J}$	Monte Carlo σ	$P(J=J^*)$
Con. PSO	0.7375	0.7423	2.05e-6	0.20
Con. APSO	0.7375	0.7405	2.18e-6	0.15
APSO+ Gauss	0.7375	0.7393	2.62e-6	0.35
APSO+ Singer	0.7375	0.7394	2.01e-6	0.25
APSO+ Sin	0.7375	0.7394	3.73e-6	0.20
MAPSO	**0.7375**	**0.7338**	**2.04e-6**	**0.45**

All the algorithms can retrieve the same best cost-function value (0.7375), which can be regarded as the global optima. This is achieved by a powertrain using a 2.1L engine-generator, a battery pack with 82 modules and power distribution function coefficient of 0.18. It shows that the modified PSO algorithm can obtain the optimization results with mixed-integer variables. The mean values and standard deviations of the cost-function values obtained by the MAPSO and APSOs with CAS are smaller than the conventional PSO and APSO. MAPSO achieves the minimum mean value (0.7338). APSO with Singer strategy attains the lowest standard deviation value (2.01e-6) followed by the MAPSO (2.04e-6). The probability of achieving the global best by the MAPSO is 0.45, which is more than twice higher than the conventional PSO ($P(J=J^*)$=0.2).

The comprehensive reputation scoring system is established based on the ranking of each algorithm in terms of its Monte Carlo results (i.e. mean cost function value $\bar{J}$ and its standard derivation σ) and the probability of achieving global optima $P(J=J^*)$. The higher the ranking the algorithm has, the higher comprehensive reputation score (CRS) it will gain, e.g., for each evaluation index, the algorithm with the 1st ranking scores 6, and the 6th ranking algorithm scores 1. The scoring of the six optimization methods is shown in Fig. 6. , and the proposed MAPSO is considered as the best for modular design, gaining a CRS of 17 which is more than twice higher than the conventional PSO (CRS=8).

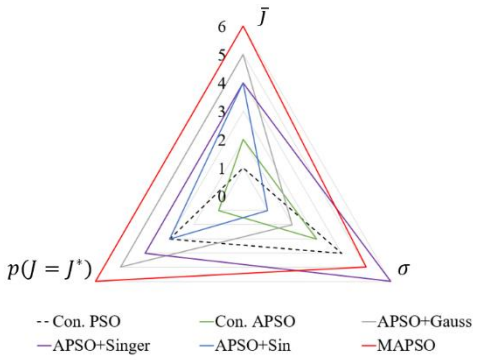

Fig. 6. Scoring of the optimization methods

C. Powertrain Performance with the Optimal Parameters

The powertrain performance using the design parameters obtained by both two-level and simultaneous methods are obtained in Fig.7. The experiment is carried out in the combined cycle on the hardware-in-the-loop platform. The results obtained with the simultaneous method are shown in purple, and the results obtained using two-level methods with initial control parameter guess of 0.05, 0.10 and 0.20, are shown in blue, red, yellow, respectively.

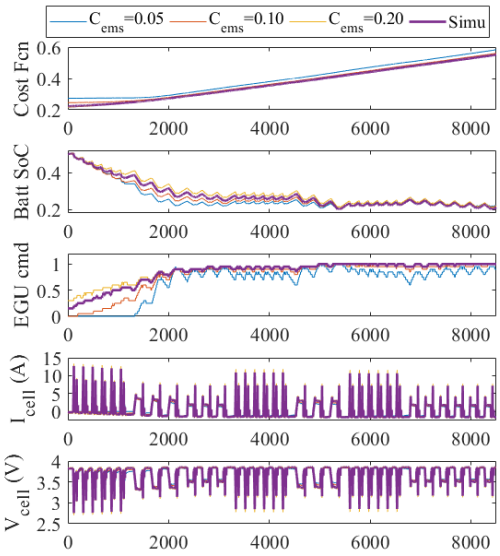

Fig. 7. Powertrain performance in the combined cycle

The results indicate that the hybrid powertrain with the optimized parameters works appropriately: the engine-generator can provide enough power to maintain the battery SoC. In all the given cases, the battery pack can supply enough power, while the voltage and current are within their safe limits. The two-level optimization highly depends on the initial guess on control parameters, the two-level method with initial $C_{ems}=0.20$ achieves the lowest cost-function value of 0.5621, 4.8% better than the two-level optimisation with initial $C_{ems}=0.05$. The simultaneous method does not need an initial guess, while it can achieve a cost-function value of 0.5595. In terms of the computational efforts, the average time for the simultaneous optimization in 20 trials is 365.37s, and it requires 732.27s for the two-stage method on the same PC. Only three variables are considered for simplification in this work, but the contribution on timesaving is expected to grow exponentially while the design variables in real practice can be more than hundreds.

D. Robustness of the Modular Design Results

To evaluate the robustness of the optimization results, tests under four different driving cycles are carried out on the hardware-in-the-loop (HiL) platform. The cost-function values affecting the performance of the optimization are listed in Table V. In general, the simultaneous method can achieve better (lower) cost function values compared to the two-stage methods with different initial guesses of the control parameter. Under the combined cycle (was used for offline optimization), the cost function value at the end of the HiL test with the results of the simultaneous optimization is 0.5508, which is 5.8% better than that obtained by the two-level method ($c_{ems}=0.05$). The reductions of 2.4%, 3.17%, and 7.5% in cost function values have been achieved by the simultaneous method compared to the two-level method ($c_{ems}=0.05$) under RWC1, 2, and 3,

respectively. This indicates the simultaneous method has higher potential in cost-function value reduction in the driving cycles with higher average power demand. We can also conclude that the simultaneous method with MAPSO outperforms the two-level methods robustly in the defined driving cycles.

Table V. VEHICLE ENERGY CONSUMPTION IN DIFFERENT CYCLES

Cycle Name	Method	Cost-fcn value
Combined cycle	Two-level (c=0.05)	0.5905
	Two-level (c=0.1)	0.5813
	Two-level (c=0.2)	0.5621
	Simultaneous	***0.5595***
Real-world cycle 1	Two-level (c=0.05)	0.4043
	Two-level (c=0.1)	0.4016
	Two-level (c=0.2)	0.3982
	Simultaneous	***0.3944***
Real-world cycle 2	Two-level (c=0.05)	0.3799
	Two-level (c=0.1)	0.3760
	Two-level (c=0.2)	0.3717
	Simultaneous	***0.3682***
Real-world cycle 3	Two-level (c=0.05)	0.4250
	Two-level (c=0.1)	0.4137
	Two-level (c=0.2)	0.3981
	Simultaneous	***0.3953***

VI. CONCLUSIONS

This paper proposes a modular design method for hybrid powertrain with a Modified Accelerated Particle Swarm optimization (MAPSO) algorithm. The probability of achieving the globally optimal result is improved by the chaotic attraction strategy. Experimental studies have been carried out on both software-in-the-loop and hardware-in-the-loop platforms. The conclusions drawn from the investigation are:

- Introducing a weighting value (changing from 0 to 1) in the MAPSO algorithm allows the designer to investigate the sensitivity of the two optimization objectives based on the Pareto frontier. Higher reduction rate in energy loss can be achieved with less increase of powertrain size when the weighting factor is lower than 0.75.
- Introducing a 'floor' function enables the MAPSO algorithms with the capability of optima searching in discrete-varying domains. The proposed MAPSO algorithm has shown robustness in achieving the same best result compared with conventional PSO, conventional APSO, and the APSOs with three other chaos maps.
- The MAPSO with logistic chaotic attraction strategy is proven as the most effective under the comprehensive reputation scoring scheme. It has the highest CRS of 17 which is at least twice higher than the conventional PSO.
- MAPSO is compatible with both two-level and simultaneous optimization methods. Compared to the two-level method, the simultaneous method can achieve 7% better cost function value with 50% less time-consuming.

In the future, the proposed modular design method will be integrated with digital twin models to globally optimize the energy efficiency and safety of connected vehicles.

APPENDIX I VEHICLE MODEL

The aircraft-towing tractor is modelled backwards with the speed profile of driving cycles to calculate the force demand

$$F_{\mathrm{dem}} = F_a + F_d + F_f \tag{A1}$$

where $F_a = (m_{\mathrm{veh}} + m_{\mathrm{plane}}) \cdot \frac{\dot{v_d}}{3.6}$, $F_d = \frac{C_d \cdot A_f \cdot {v_d}^2}{21.15}$, and $F_f = (m_{\mathrm{veh}} + m_{\mathrm{plane}}) \cdot g \cdot f_f$ are acceleration resistance, air drag, and friction resistance; m_{veh} and m_{plane} are the mass of the tractor and the airplane in kg; v_d is the vehicle speed in km/h; m_{plane} and v_d are defined by driving cycles; C_d and f_f are the drag and rolling resistance coefficient; A_f is the front area of the tractor; and g is gravity constant. Because the tractor is working on flat grounds, the climbing resistance is ignored. The power and energy demand of the powertrain are calculated by

$$\left.\begin{aligned} P_{\mathrm{dem}} &= \frac{F_{\mathrm{dem}} \cdot v_d}{\eta_{\mathrm{tran}} \cdot \eta_{\mathrm{m}}(n_m, T_m)} \\ E_{\mathrm{dem}} &= \int_{t=t_0}^{t_t} P_{\mathrm{dem}}(t)\, dt \end{aligned}\right\} \tag{A2}$$

where η_{tran} is the efficiency of the transmission which is 0.95 according to the datasheet from the supplier; η_{m} is the efficiency of traction motor, which is a two-dimensional map of motor speed n_m and torque T_m [17]; and t_0 and t_t are the start time and terminate time in a driving cycle.

APPENDIX II NOMENCLATURE

P_{fuel}	Equivalent power for fuel consumption	P_{dem}	Vehicle's power demand
L_{ice}	Displacement of the engine	c_{ems}	Control parameters
u_{egu}	Engine-generator control command	$\boldsymbol{\mathcal{L}}$	A set of candidates L_{ice}values
vol_{egu}	Dimensional size of the engine-generator	$\boldsymbol{\mathcal{N}}$	A set of candidates n_{bm}values
n_{bm}	Number of battery modules	$\boldsymbol{\mathcal{C}}$	A set of candidates c_{ems}values
R_{eqv}	Battery internal resistance	p	Population of the particles
I_{batt}	Battery module current	n	The maximum iteration number
U_{batt}	Battery module voltage	β	Attraction factor
r_{cell}	Radius of the battery cell	μ	Tuning parameter in the logistic map
h_{cell}	Height of the battery cell	ER	Error ratio
P_{batt}	Power supplied by the battery pack	GD	Generational distance
P_{egu}	Power of the engine-generator		

ACKNOWLEDGEMENT

The authors acknowledge to the support from the Innovate UK (102253), the EPSRC Fellowship (EP/S001956/1), and the State Key Laboratory of Automotive Safety and Energy, Tsinghua University (KF2029).

REFERENCE

[1] E. Gregor, "EU Legislation in Progress CO 2 emission standards for heavy-duty vehicles," no. December 2018, 2019.

[2] European Commission, "Proposal for post-2020 CO2 targets for cars and vans | Climate Action," 2017. .

[3] C. Lv, J. Zhang, Y. Li, and Y. Yuan, "Mechanism analysis and evaluation methodology of regenerative braking contribution to energy efficiency improvement of electrified vehicles," *Energy Convers. Manag.*, vol. 92, pp. 469–482, 2015.

[4] Q. Zhou, X. Guo, G. Tan, X. Shen, Y. Ye, and Z. Wang, "Parameter Analysis on Torque Stabilization for the Eddy Current Brake: A Developed Model, Simulation, and Sensitive Analysis," *Math. Probl. Eng.*, vol. 2015, pp. 1–10, 2015.

[5] S. Guo, Z. Chen, X. Guo, Q. Zhou, and J. Zhang, "Vehicle Interconnected Suspension System based on Hydraulic Electromagnetic Energy Harvest: Design, Modeling and Simulation Tests," *SAE Tech. Pap. 2014-01-2299*, 2014.

[6] C. M. Martinez, X. Hu, D. Cao, E. Velenis, B. Gao, and M. Wellers, "Energy Management in Plug-in Hybrid Electric Vehicles: Recent Progress and a Connected Vehicles Perspective," *IEEE Trans. Veh. Technol.*, vol. 66, no. 6, pp. 4534–4549, Jun. 2017.

[7] F. Zhang, X. Hu, R. Langari, and D. Cao, "Energy management strategies of connected HEVs and PHEVs: Recent progress and outlook," *Prog. Energy Combust. Sci.*, vol. 73, pp. 235–256, 2019.

[8] Y. He *et al.*, "Multiobjective Co-Optimization of Cooperative Adaptive Cruise Control and Energy Management Strategy for PHEVs," *IEEE Trans. Transp. Electrif.*, vol. 6, no. 1, pp. 346–355, 2020.

[9] Y. Huang, H. Wang, A. Khajepour, H. He, and J. Ji, "Model predictive control power management strategies for HEVs: A review," *J. Power Sources*, vol. 341, pp. 91–106, 2017.

[10] Q. Zhou *et al.*, "Cyber-Physical Energy-Saving Control for Hybrid Aircraft-Towing Tractor based on Online Swarm Intelligent Programming," *IEEE Trans. Ind. Informatics*, vol. 14, no. 9, pp. 4149–4158, 2018.

[11] D. Zhao, R. Stobart, G. Dong, and E. Winward, "Real-Time Energy Management for Diesel Heavy Duty Hybrid Electric Vehicles," *IEEE Trans. Control Syst. Technol.*, vol. 23, no. 3, pp. 829–841, 2015.

[12] H. Wang, Y. Huang, H. He, C. Lv, W. Liu, and A. Khajepour, "Energy Management of Hybrid Electric Vehicles," in *Modeling, Dynamics, and Control of Electrified Vehicles*, 2017, pp. 159–206.

[13] T. Liu, X. Hu, S. E. Li, and D. Cao, "Reinforcement Learning Optimized Look-Ahead Energy Management of a Parallel Hybrid Electric Vehicle," *IEEE/ASME Transactions on Mechatronics*, vol. 22, no. 4. pp. 1497–1507, 2017.

[14] B. Shuai *et al.*, "Heuristic action execution for energy efficient charge-sustaining control of connected hybrid vehicles with model-free double Q-learning," *Appl. Energy*, vol. 267, no. 2020, 2020.

[15] Q. Zhou *et al.*, "Multi-step Reinforcement Learning for Model-Free Predictive Energy Management of an Electrified Off-highway Vehicle," *Appl. Energy*, vol. 255, no. 2019, pp. 588–601, 2019.

[16] Y. Huang *et al.*, "A review of power management strategies and component sizing methods for hybrid vehicles," *Renew. Sustain. Energy Rev.*, vol. 96, pp. 132–144, Nov. 2018.

[17] Q. Zhou *et al.*, "Intelligent sizing of a series hybrid electric power-train system based on Chaos-enhanced accelerated particle swarm optimization," *Appl. Energy*, vol. 189, pp. 588–601, 2017.

[18] B. Schwambach *et al.*, "Conceptualization and Implementation of a Scalable Powertrain, Modular Energy Storage and an Alternative Cooling System on a Student Concept Vehicle," in *SAE Technical Papers*, 2018, vol. 2018-April, pp. 1–14.

[19] "The modular electric drive matrix," *Volkswagen AG*, 2019. .

[20] "Changan Open New Test Centre and Unveil Blue Core 1.5T Engine," *Changan UK R&D Centre Ltd.*, 2019. .

[21] "SAE Truck & Off-Highway Engineering: December 2019," *SAE International*, Dec-2019.

[22] A. E. Bayrak, A. X. Collopy, B. I. Epureanu, and P. Y. Papalambros, "A computational concept generation method for a modular vehicle fleet design," *10th Annu. Int. Syst. Conf. SysCon 2016 - Proc.*, pp. 1–8, 2016.

[23] Y. Huang *et al.*, "A review of power management strategies and component sizing methods for hybrid vehicles," *Renew. Sustain. Energy Rev.*, vol. 96, no. April 2017, pp. 132–144, 2018.

[24] E. Silvas, T. Hofman, N. Murgovski, L. F. P. Etman, and M. Steinbuch, "Review of Optimization Strategies for System-Level Design in Hybrid Electric Vehicles," *IEEE Trans. Veh. Technol.*, vol. 66, no. 1, pp. 57–70, 2017.

[25] M. Pourabdollah, B. Egardt, N. Murgovski, and A. Grauers, "Convex Optimization Methods for Powertrain Sizing of Electrified Vehicles by Using Different Levels of Modeling Details," *IEEE Trans. Veh. Technol.*, vol. 67, no. 3, pp. 1881–1893, 2018.

[26] L. Zhang, X. Hu, Z. Wang, F. Sun, J. Deng, and D. G. Dorrell, "Multiobjective Optimal Sizing of Hybrid Energy Storage System for Electric Vehicles," *IEEE Trans. Veh. Technol.*, vol. 67, no. 2, pp. 1027–1035, 2018.

[27] M. Shahverdi, M. S. Mazzola, Q. Grice, and M. Doude, "Pareto Front of Energy Storage Size and Series HEV Fuel Economy Using Bandwidth-Based Control Strategy," *IEEE Trans. Transp. Electrif.*, vol. 2, no. 1, pp. 36–51, 2016.

[28] X. Xu, H. Sun, Y. Liu, and P. Dong, "Automatic Enumeration of Feasible Configuration for the Dedicated Hybrid Transmission with Multi-Degree-of-Freedom and Multiplanetary Gear Set," *J. Mech. Des. Trans. ASME*, vol. 141, no. 9, pp. 1–14, 2019.

[29] X. Wang and Q. Liang, "Energy management strategy for plug-in hybrid electric vehicles via bidirectional vehicle-to-grid," *IEEE Syst. J.*, vol. 11, no. 3, pp. 1789–1798, 2017.

[30] C. Lv *et al.*, "Levenberg-marquardt backpropagation training of multilayer neural networks for state estimation of a safety-critical cyber-physical system," *IEEE Trans. Ind. Informatics*, vol. 14, no. 8, pp. 3436–3446, 2018.

[31] C. Lv, X. Hu, A. Sangiovanni-Vincentelli, Y. Li, C. M. Martinez, and D. Cao, "Driving-Style-Based Codesign Optimization of an Automated Electric Vehicle: A Cyber-Physical System Approach," *IEEE Trans. Ind. Electron.*, vol. 66, no. 4, pp. 2965–2975, 2019.

[32] N. Leahey and J. Bauman, "A fast plant-controller optimization process for mild hybrid vehicles," *IEEE Trans. Transp. Electrif.*, vol. 5, no. 2, pp. 444–455, 2019.

[33] A. Al Mamun, Z. Liu, D. M. Rizzo, and S. Onori, "An integrated design and control optimization framework for hybrid military vehicle using lithium-ion battery and supercapacitor as energy storage devices," *IEEE Trans. Transp. Electrif.*, vol. 5, no. 1, pp. 239–251, 2019.

[34] B. Anvari, H. A. Toliyat, and B. Fahimi, "Simultaneous Optimization of Geometry and Firing Angles for In-Wheel Switched Reluctance Motor Drive," *IEEE Trans. Transp. Electrif.*, vol. 4, no. 1, pp. 322–329, 2017.

[35] M. J. Kim and H. Peng, "Power management and design optimization of fuel cell/battery hybrid vehicles," *J. Power Sources*, vol. 165, no. 2, pp. 819–832, 2007.

[36] S. Guo, M. Dooner, J. Wang, H. Xu, and G. Lu, "Adaptive Engine Optimisation Using NSGA-II and MODA Based on a Sub-Structured Artificial Neural Network," no. September, pp. 7–8, 2017.

[37] H. Ma *et al.*, "Model-based Multi-objective Evolutionary Algorithm Optimization for HCCI Engines," *IEEE Trans. Veh. Technol.*, vol. 9545, no. c, pp. 1–1, 2014.

[38] H. Ma, Z. Li, M. Tayarani, G. Lu, H. Xu, and X. Yao, "Computational Intelligence Non-model-based Calibration Approach for Internal Combustion Engines," *J. Dyn. Syst. Meas. Control*, vol. 140, no. April, pp. 1–9, 2017.

[39] Y. Zhang, Q. Zhou, Z. Li, J. Li, and H. Xu, "Intelligent transient calibration of a dual-loop EGR diesel engine using chaos-enhanced accelerated particle swarm optimization algorithm," *Proc. Inst. Mech. Eng. Part D J. Automob. Eng.*, 2018.

[40] J. Li, Q. Zhou, H. Williams, and H. Xu, "Back-to-back Competitive Learning Mechanism for Fuzzy Logic based Supervisory Control System of Hybrid Electric Vehicles," *IEEE Trans. Ind. Electron.*, pp. 1–1, 2019.

[41] J. Kennedy and R. Eberhart, "Particle swarm optimization," in *Proceedings of ICNN'95 - International Conference on Neural Networks*, 1995, vol. 4, pp. 1942–1948.

[42] X.-S. Yang, "Particle Swarm Optimization," in *Nature-Inspired Optimization Algorithms*, Elsevier, 2014, pp. 99–110.

[43] J. Wan, L. Ding, J. Yao, and H. Wu, "A hybrid CHAOS-PSO algorithm for dimensional synthesis of a redundant manipulator based on tracking trajectories without or with singularities," *Prod. Eng.*, vol. 12, no. 5, pp. 579–587, 2018.

[44] L. Y. Chuang, C. J. Hsiao, and C. H. Yang, "Chaotic particle swarm optimization for data clustering," *Expert Syst. Appl.*, vol. 38, no. 12, pp. 14555–14563, 2011.

[45] Z. Li, Q. Zhou, Y. Zhang, J. Li, and H. Xu, "Enhanced intelligent proportional-integral-like fuzzy knowledge–based controller using chaos-enhanced accelerated particle swarm optimization algorithm for transient calibration of air–fuel ratio control system," *Proc. Inst. Mech. Eng. Part D J. Automob. Eng.*, p. 095440701986207, 2019.

[46] Y. Yu, G. Pu, T. Jiang, and K. Jiang, "Discontinuous grooves in thrust air bearings designed with CAPSO algorithm," *Int. J. Mech. Sci.*, vol. 165, no. September 2019, p. 105197, 2020.

[47] A. H. Gandomi, G. J. Yun, X.-S. Yang, and S. Talatahari, "Chaos-enhanced accelerated particle swarm optimization," *Commun. Nonlinear Sci. Numer. Simul.*, vol. 18, no. 2, pp. 327–340, Feb. 2013.

[48] Di He, Chen He, Ling-Ge Jiang, Hong-Wen Zhu, and Guang-Rui Hu, "Chaotic characteristics of a one-dimensional iterative map with infinite collapses," *IEEE Trans. Circuits Syst. I Fundam. Theory Appl.*, vol. 48, no. 7, pp. 900–906, Jul. 2001.
[49] I. Fister, M. Perc, S. M. Kamal, and I. Fister, "A review of chaos-based firefly algorithms: Perspectives and research challenges," *Appl. Math. Comput.*, vol. 252, pp. 155–165, Feb. 2015.
[50] Y. Li, S. Deng, and D. Xiao, "A novel Hash algorithm construction based on chaotic neural network," *Neural Comput. Appl.*, vol. 20, no. 1, pp. 133–141, Feb. 2011.
[51] "JCB Generator Technical Specifications," *JCB Power Products*, 2015. [Online]. Available: http://www.midas-uk.com/PDF/JCB/QS/G116QS_EN.pdf.
[52] "Lithium Ion Battery-Cylindrical, Type: UR-18650," *Panasonic Automotive & Industrial Systems Europe GmbH*, 2017. [Online]. Available: https://eu.industrial.panasonic.com/products/batteries-energy-products/secondary-batteries-rechargeable-batteries/lithium-ion-batteries/series/cylindrical-type/ACI4002/model/UR-18650E.
[53] B. Chopard and M. Tomassini, "Particle swarm optimization," in *Natural Computing Series*, Elsevier, 2018, pp. 97–102.
[54] K. Deb, *Multi-Objective Optimization Using Evolutionary Algorithms*. New York: John Wiley & Sons, 2001.

Quan Zhou (M'17) received the Ph.D. degree in mechanical engineering from the University of Birmingham (UoB) in 2019 that was distinguished by being the school's solo recipient of the UoB's Ratcliffe Prize of the year. He is currently a Research Fellow and leads the Connected and Autonomous Systems for Electrified Vehicles (CASE-V) Research at UoB. His research interests include evolutionary computation, fuzzy logic, reinforcement learning, and their application in vehicular systems. One of Dr Zhou's research outcomes has been awarded an Innovate U.K. grant for commercialization of university research. He received a visiting scholar award from Tsinghua University, in 2019, for leading a project that develops digital twin for electrified powertrains. He reviews articles for Applied Energy and the IEEE transactions.

Yinglong He received the B.Eng. and M.Res. degrees in energy and power engineering from Huazhong University of Science and Technology, Wuhan, China, in 2014 and 2017, respectively. He is currently a scholarship-funded Ph.D. candidate with the CASE-V Team at UoB. His research interests include intelligent transportation, vehicle dynamics, driver behaviors, multi-objective optimization and machine learning.

Dezong Zhao (M'12–SM'17) received the B.Eng. and M.S. degrees from Shandong University, Jinan, China, in 2003 and 2006, respectively, and the Ph.D. degree from Tsinghua University, Beijing, China, in 2010, all in Control Science and Engineering. Since 2017, he has been a Lecturer with the Department of Aeronautical and Automotive Engineering, Loughborough University (LU), U.K. Dr Zhao's research interests include connected and autonomous vehicles, machine learning and control engineering. His work has been recognized by being awarded an EPSRC Fellowship and a Royal Society-Newton Advanced Fellowship in 2018 and 2020, respectively.

Ji Li (M'19) received the B.S. degree (Hons) in vehicle engineering from the Chongqing University of Technology, Chongqing, China, in 2015. He is currently working toward the Ph.D. degree with the CASE-V team at UoB. His current research interests include fuzzy mathematics, meta-heuristic algorithms, deep reinforcement learning, and man-machine system for intelligent vehicles.

Yanfei Li received the B. Eng. in Power Machinery from Jilin University, Changchun, China, in 2006 and Ph.D. degree in Mechanical Engineering from University of Birmingham, Birmingham, United Kingdom in 2012. He is currently a research-focused Assistant Professor at the State Key Laboratory of Automotive Safety and Energy, Tsinghua University, Beijing, China. His research interests include emissions and two-phase flows in the internal combustion engines (ICE), and dedicated ICE design for hybrid vehicles.

Huw Williams is an honorary professor at the UoB and the director of DEEPPOWER Innovation Ltd. (a university spin-off). He is a professional mathematician with excellent skills in Lean, Six Sigma, Engineering Physics and Statistics. Huw has over 20 years' experience in the automotive industry; he graduated from the University of Oxford in 1978 with a mathematics degree and went on to take a PhD in theoretical mechanics at the University of East Anglia. Huw joined Jaguar Land Rover (JLR) in 1986 and then become one of only two people to hold the position of Senior Engineering Specialist in JLR's product development organization. He also developed statistical skills through TQM in the 1980's culminating in his accreditation as Ford's top-scoring Master Black Belt in 2005.

Hongming Xu received the Ph.D. degree in mechanical engineering from Imperial College London, London, U.K. He is a Professor of Energy and Automotive Engineering at the University of Birmingham, Birmingham, U.K., and the Head of Vehicle and Engine Technology Research Centre. He has six years of industrial experience with Jaguar Land Rover and Premier Automotive Group of Ford. He has authored and co-authored more than 300 journal and conference publications on advanced vehicle powertrain systems involving both experimental and modeling studies. Prof. Xu was a member of the Ford HCCI Global Steering Committee, a Project Manager and Technical Leader of U.K. Foresight Vehicle LINK projects CHARGE and CHASE from 2002 to 2007. He is a Fellow of SAE International and IMechE.